

Robot-Assisted and Wearable Sensor-Mediated Autonomous Gait Analysis[§]

Huanghe Zhang[†], *Student Member, IEEE*, Zhuo Chen[‡], *Student Member, IEEE*,
Damiano Zanotto^{*†}, *Member, IEEE*, Yi Guo[‡], *Senior Member, IEEE*

Abstract—In this paper, we propose an autonomous gait analysis system consisting of a mobile robot and custom-engineered instrumented insoles. The robot is equipped with an on-board RGB-D sensor, the insoles feature inertial sensors and force sensitive resistors. This system is motivated by the need for a robot companion to engage older adults in walking exercises. Support vector regression (SVR) models were developed to extract accurate estimates of fundamental kinematic gait parameters (i.e., stride length, velocity, foot clearance, and step length), from data collected with the robot’s on-board RGB-D sensor and with the instrumented insoles during straight walking and turning tasks. The accuracy of each model was validated against ground-truth data measured by an optical motion capture system with N=10 subjects. Results suggest that the combined use of wearable and robot’s sensors yields more accurate gait estimates than either sub-system used independently. Additionally, SVR models are robust to inter-subject variability and type of walking task (i.e., straight walking vs. turning), thereby making it unnecessary to collect subject-specific or task-specific training data for the models. These findings indicate the potential of the synergistic use of autonomous mobile robots and wearable sensors for accurate out-of-the-lab gait analysis.

Index Terms—Wearable Technology, Instrumented Footwear, Gait Analysis, Assistive Robotics, SportSole

I. INTRODUCTION

An active lifestyle can mitigate physical and cognitive decline in the elderly, thus preserving their independence [1]. Walking programs are routinely offered in senior centers [2], since they may result in enhanced balance and muscle strength as well as reduced risk of falling [3]. However, the increasing shortage of trained caregivers due to population aging and increased life expectancy is posing a serious threat to the sustainability of such initiatives in the future [4].

Moreover, because alterations in walking patterns may be markers of frailty, precursors of falls, and indicators of neurological or musculoskeletal disorders, gait assessments are often included within health screening for the elderly [5]–[7]. In this light, quantitative gait analysis may yield higher diagnostic power than traditional screening based on clinical observation and timed mobility tests [8], nonetheless it requires costly equipment (e.g., optical motion capture systems, treadmills instrumented with force plates, electronic

walkways) which limit its use to constrained laboratory environments and elite outpatient clinics. *Robotics and wearable technology can be leveraged to make supervised gait exercises and quantitative gait assessments more accessible to the rapidly increasing number of older adults.*

Several research groups have proposed the use of mobile robots equipped with either laser range sensors (LRS) [9]–[12] or RGB-D sensors [13], [14] for autonomous gait analysis. The rationale behind these applications is that robots may provide added mobility, thus making it possible to conduct self-administered gait exercises and gait assessments in patients’ living environments. Compared to RGB-D sensors, LRSs feature higher sample rates and are more robust to variability in light conditions and user’s clothes [9]. Yet, typical two-dimensional (2D) LRSs can only sense planar information at a fixed height [15], which makes them unsuitable for the estimation of 3D stride-to-stride foot parameters, such as foot clearance. On the other hand, RGB-D sensors can generate 3D representations of the whole body, from which joint angles can be extracted [16]. However, the accuracy of on-board RGB-D sensors depends on the relative distance between the subject and the robot [13], [17], [18], and common software packages for skeletal tracking based on RGB-D sensors are prone to errors and misdetections. Furthermore, significant occlusions and leg overlapping can occur during turning motions, which are hard to compensate and often result in degraded tracking performance of LRS [19], [20], RGB-D [21], and similar sensors [22]. For these reasons, despite recent efforts, neither LRS-based nor RGB-D-based systems can guarantee a level of accuracy that is suitable for quantitative gait analysis.

Wearable sensors have also been proposed in recent years as alternatives to laboratory equipment for ubiquitous and affordable gait analysis. Among those, in-shoe devices are promising since they are affordable, easy to don/doff, and allow for minimally obtrusive measurements of different tasks (e.g., ground-level walking, running, stairs negotiation, etc.) over extended time [23]. This type of devices has been validated in studies with healthy [24], [25] and clinical [26]–[30] populations. Unlike camera-based sensors, in-shoe devices can capture kinetic parameters (e.g., center of pressure) and their high sampling rate and ideal sensor location make them more accurate in estimating gait events (such as initial contact and toe-off), from which temporal parameters are extracted [31]. However, in-shoe devices typically cannot measure inter-limb spatial parameters such as step length, which is associated with fall risk [9], [18].

[§]This work was supported by the US National Science Foundation under Grant IIS-1838799.

^{*}Corresponding author (dzanotto@stevens.edu).

[†]H. Zhang and D. Zanotto are with Wearable Robotic Systems (WRS) Lab, Stevens Institute of Technology, Hoboken, NJ 07030, USA.

[‡]Z. Chen and Y. Guo (yguo1@stevens.edu) are with Robotics and Automation Lab., Stevens Institute of Technology, Hoboken, NJ 07030, USA.

More importantly, their accuracy is negatively affected by drift in the embedded inertial sensors, which negatively affects position and orientation estimates, especially during extended-time measurements [24].

To address these limitations, the *concurrent* use of wearable sensors and robot on-board sensors has been studied for human motion tracking in large environments [32], semantic mapping [33] or robot-human following [34]. The system proposed in [34], for example, is capable of measuring pelvis orientation and velocity, as well as inter-leg distance, using the integration of LRS and a wearable sensor. However, only a paucity of studies has proposed the use of *advanced machine learning* methods to fuse data from *wearable* and *mobile robot sensors* with the goal of increasing the accuracy of the estimated gait parameters.

In this paper, we propose a novel mobile gait measurement system consisting of an autonomous mobile robot equipped with an RGB-D sensor and custom-engineered instrumented insoles. We hypothesized that the synergistic use of in-shoe inertial and piezo-resistive sensors and robot on-board RGB-D sensor would improve the accuracy of either subsystem, if used individually. Our fusion approach uses the raw estimates of gait parameters obtained from instrumented insoles and from the robot as well as inertial features and subjects' anthropometric characteristics as inputs to learning-based regression models (SVR) to improve accuracy. The system was validated by conducting straight walking and turning tests with a convenience group of healthy adults, while their gait was simultaneously measured by the proposed autonomous system and by reference equipment. For each gait parameter considered (i.e., stride and step length, foot clearance, and walking speed), estimates were computed under four conditions: (i) robot-only, (ii) insoles-only, (iii) insoles-and-robot with least absolute shrinkage and selection operator (LASSO), and (iv) insoles-and-robot with SVR. LASSO models were included in the analysis to verify that the complexity of SVR models is well-justified by their superior accuracy relative to linear models. Accuracy was compared across the four conditions by determining the root-mean-square errors (RMSE) with respect to the ground-truth values using *leave-one-out* cross-validation [35]. The experimental results validate the hypothesis that the synergistic use of the robot sensors and the insoles improves the accuracy of either subsystem used alone, and also demonstrate that the SVR method achieves better accuracy than LASSO. The contributions of this work are:

- a mobile gait measurement system consisting of a mobile robot and custom-engineered instrumented insoles,
- a data fusion approach using machine learning models for accurate estimation of kinematic gait parameters, and their validation against gold-standard equipment in walking and turning tasks,
- methods for feature selection and hyperparameters tuning in the proposed machine learning models.

The rest of the paper is organized as follows. In Section II, the architecture of the mobile gait measurement system

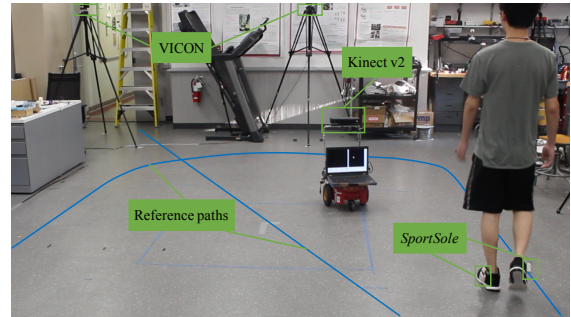


Fig. 1. The proposed system consists of custom-made instrumented insoles (*SportSole*) and a mobile robot with an on-board *Kinect v2* sensor. The optical motion-capture system (*VICON*) provides ground-truth data for validation purposes and is not part of the proposed system.

and its synchronization protocol are illustrated. Section III describes the experimental protocol. Gait analysis models are described in Section IV. Results are presented in Section V and discussed in Section VI. Finally, the paper is concluded in Section VII.

II. SYSTEM DESCRIPTION

As shown in Fig. 1, the mobile gait measurement system consists of instrumented footwear previously developed by our group (*SportSole* system, [36]–[38]) and a mobile robot equipped with *Kinect v2*. The instrumented footwear includes two insole modules and a data logger. Each insole module consists of a multi-cell piezo-resistive sensor and an IMU, both sandwiched between layers of abrasion-resistant foam, and a logic unit housed in a custom plastic enclosure that is secured to the postero-lateral side of the user's shoes with a plastic clip. The overall thickness of the instrumented insole (4.5 mm) is comparable to that of a regular insole, and the total weight of the logic unit is less than 50 g. Thus, the insole is minimally obtrusive for the user. Data measured by each insole is sent wirelessly (UDP over WLAN, 500 Hz) to a single-board Linux computer running the data logger software. For this application, the single-board computer is secured to the robot's frame along with a portable Wi-Fi router, which served as an access point.

The robot subsystem consists of an RGB-D sensor (*Kinect v2*), a laptop computer, and a P3-DX robot. The *Kinect v2* is attached to the robot at the height of 0.7 meters from the ground, facing backward (i.e., toward the subject), to keep track of the movement of the subject's ankle joints. We used the *Kinect SDK 2.0* [39] to extract 3D position coordinates of the subject's ankle joints from depth image data captured at 30 Hz. Custom code running in the laptop computer transforms the ankle position measurements from the *Kinect* frame to the robot frame, and logs the data for subsequent offline gait parameters calculation.

The P3-DX robot is a differential-drive robot with two driving wheels in the front and one caster wheel at the back. The robot follows a predefined path (i.e., straight line, counterclockwise, or clockwise paths) by using the path following control law presented in [40]. The control law takes the desired speed of the robot as an input, which is

FAMILIARIZATION SESSION	CLOCKWISE CURVED WALKING	COUNTERCLOCKWISE CURVED WALKING	STRAIGHT WALKING
2~5 mins	2 mins	2 mins	10 reps

Fig. 2. Experimental protocol. The sequence of each task was randomized.

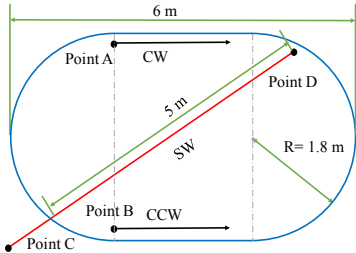


Fig. 3. Reference paths for the CW and CCW tasks (blue oval shape) and for the SW task (red straight line). Starting points for each tasks are marked as A, B, and C, respectively.

prescribed such that it is higher in the straight portion of the path but lower while the robot is cornering because the subject needs to track an arc of larger radius than that of the robot to follow the reference paths (Fig. 1). The controller relies on wheel odometry to obtain the robot pose feedback. This solution is deemed appropriate, since the expected drift is minimal due to the short duration of the walking trials (explained in the next section) and the predefined path and speed of the robot.

Reference Broadcast Time Synchronization [41] was used to synchronize all the devices in the system. To this end, the data logger broadcasts its internal timestamp to all the nodes in the network at 1 Hz, and this reference is used to adjust the internal timestamps of all devices.

III. EXPERIMENTAL PROTOCOL

$N=10$ healthy male adults (age 24.3 ± 3.5 years, weight 68.6 ± 7.4 kg, height 1.73 ± 0.04 m and US shoe size 8.9 ± 0.6) volunteered for this experiment, designed as an initial proof-of-concept validation of the mobile gait measurement system.

Prior to testing, each subject chose an appropriate insole size among the four sizes available, and then fit the instrumented insoles in his shoes. Reflective markers were placed on the subject's shoes, close to the hallux, the calcaneus, and the heads of the first, second, and fifth metatarsal. An optical motion capture system (VICON Vero v2.2, Oxford, U.K.) with eight cameras was used to track the markers during data collection (Fig. 1). The centroid of the markers attached to each shoe was used to estimate foot displacement. After the system setup, participants were instructed to complete a familiarization session. During this session, subjects were asked to follow the robot, while keeping a distance of 1.5m to 2.5m from the robot. After the familiarization session, subjects were instructed to follow the robot to complete a clockwise curved walking (CW) task, a counterclockwise curved walking (CCW) task, and 10 repetitions of straight walking (SW) task (Fig. 2). The sequence of these tasks was randomized.

For each walking task, the corresponding prescribed path for the subject was marked on the floor (Fig. 1). CW and

CCW tasks were carried out on an oval track, shown in Fig. 3, starting from point A and B, respectively. For SW task, subjects were asked to walk from point C (located approximately 2 meters outside the oval path) to point D. Only the last 5m of the straight-line path were included in the analysis.

Before each task, subjects were asked to stand still for 5 seconds while the system was initialized. The IMU embedded in the insoles, as well as the robot's gyroscope, were zeroed at this time, and never reset during each walking task. Gait parameters were simultaneously recorded by the mobile gait measurement system and by the optical motion-capture system. A custom-made wireless board working at 500 Hz was used to synchronize the optical motion-capture system and the mobile gait analysis system, by relaying a TTL-compatible sync output from the reference system to the data logger [36].

IV. SVR MODELS AND FUSION ALGORITHM

In this section, we present a novel 2-step fusion approach to improve the estimates of stride-to-stride gait parameters obtained with the proposed mobile gait measurement system. The first step is to obtain raw stride-to-stride gait parameter estimations from both subsystems (i.e., the robot's on-board Kinect sensor and the insoles). The second step consists in using the raw estimations from the two subsystems, as well as inertial features from insoles and subjects' anthropometric characteristics, as inputs to SVR models, to improve the accuracy of gait estimations. For each gait parameter, the accuracy of the proposed SVR model was compared to that of a simple linear model (LASSO).

A. Support Vector Regression (SVR)

Machine learning models are expected to be more effective than linear models in reducing estimation errors in complex datasets, due to their vast expressive power [42]. For this reason, we apply SVR models to combine the robot data with instrumented insoles data. SVR models estimate the i -th gait parameter \hat{p}_i as

$$\hat{p}_i = f(X_i, \beta) = \beta^T \Phi(X_i) \quad (1)$$

where $\Phi(X)$ is the kernel function, mapping the set of input features at the i -th stride, X_i , to a high-dimensional feature space. Candidate features include the i -th raw gait parameters estimated by the instrumented insoles p_i^I and robot p_i^R (described in Section C below), plus inertial features and subjects' anthropometric characteristics (described in Section D). The weights vector β is determined by numerically solving the constrained convex optimization problem:

$$\min \frac{\|\beta\|^2}{2} + C \sum_{i=1}^{N_s} (\xi_i + \xi_i^*) \quad (2)$$

subject to:

$$\begin{aligned} p_i^{ref} - \beta^T \Phi(X_i) &\leq \varepsilon + \xi_i^*, \quad i = 1, \dots, N_s \\ \beta^T \Phi(X_i) - p_i^{ref} &\leq \varepsilon + \xi_i, \quad i = 1, \dots, N_s \\ \xi_i, \xi_i^* &\geq 0, \quad i = 1, \dots, N_s \end{aligned} \quad (3)$$

where C is a regularization parameter that determines the importance of fitting errors relative to model complexity. N_s

is the total number of strides, p_i^{ref} is the i -th reference gait parameter, ε is the tolerance, such that errors of magnitude ε or less are neglected. The slack variables ξ_i and ξ_i^* bound regression errors that are tolerated.

B. Multivariate Linear Regression with LASSO

The LASSO is a shrinkage method that minimizes the residual sum of squares while controlling the L_1 -norm of the weights vector β . Compared to least-squares linear regression, LASSO can zero out some coefficients in β . Therefore, LASSO can be used for feature selection and to mitigate the risk of overfitting the data. The LASSO model can be described as

$$\hat{\beta} = \min_{\beta} \frac{1}{2} \sum_{i=1}^{N_s} (p_i^{ref} - \beta_0 - \sum_{j=1}^m X_{ij} \beta_j)^2 + \lambda \sum_{j=1}^m |\beta_j| \quad (4)$$

where λ is a nonnegative regularization parameter, m is the number of features, and X_{ij} is the j -th feature measured at the i -th stride. The value of λ is chosen based on 10-fold cross-validation and the “one-standard-error” rule [43].

C. Pre-processing of Raw Gait Data

The definition of the spatial gait parameters used in this paper is illustrated in Fig. 4, which follows the standard definition in [44].

The calculation of the raw gait parameters using the robot subsystem consists of three steps: footstep clustering, footstep triplet grouping, and final calculation. First, the data points collected by the Kinect sensor during foot-flat phases are clustered into individual footstrokes, using both the spatial and the temporal distances between sampled points. Then, in order for a footstep cluster to be considered as valid, the following checks are performed: 1) the number of data points within the footstep is larger than a threshold n_{th} ; 2) the duration of the corresponding foot-flat phase is less than a threshold t_1 ; 3) the temporal separation between the current and the previous foot-flat phase is larger than a threshold t_2 . Next, footstep clusters are grouped into a sequence of triplets of successive footstrokes, with each triplet being one of the two types – left-right-left or right-left-right. The final calculation is performed in accordance with the gait parameter definition shown in Fig. 4. In our implementation, we selected $n_{th} = 10$, $t_1 = 1$ s and $t_2 = 0.8$ s. These values were tuned empirically during preliminary tests with one subject, similar to [37]. Additionally, stride velocity was defined as the ratio between the stride length and the corresponding stride time. Foot clearance was defined as the maximal foot height during swing phase relative to the minimal foot height during stance phase.

The calculation of the raw gait parameters using the insoles subsystem starts from the determination of gait events, i.e., the timing of heel strike, foot-flat, heel-off and toe-off events, based on the underfoot piezo-resistive sensors, from which the stride time is also derived. Then, to obtain stride-to-stride estimates of stride length, stride velocity and foot clearance, Zero Velocity Update (ZUPT) [45] and Velocity Drift Compensation (VDC) [46] techniques are adopted, as described in our previous work [25], [28], [37], [38]. It

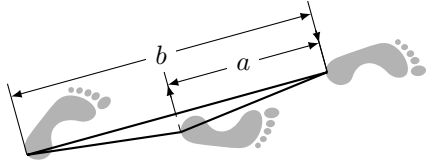


Fig. 4. Definition of spatiotemporal gait parameters in terms of the three heel points of a left-right-left footstep triplet: left step length (a) and left stride length (b).

should be noted that the use of underfoot piezo-resistive sensors to estimate temporal gait parameters (i.e., stride time and normalized swing time) has been done in existing work [31] and therefore it is not the main goal of validation.

D. Feature Extraction and Model Training

The list of candidate features is reported in Table I. Inertial features computed for each stride (i.e., between consecutive foot-flat periods of the same foot) include: norm of the foot acceleration, as well as maximum, minimum, median, root mean square, sum, energy¹, absolute sum of change², and sample entropy of the vertical (a_z) and horizontal (a_{xy}) of the foot acceleration projections. Stride time and normalized swing time were also included. The anthropometric features used in this study include height, weight, body mass index (BMI), and shoe size.

LASSO and SVR models were trained, subject by subject, using data from all the other subjects, while the excluded subject’s data formed the testing dataset (leave-one-out cross-validation). Both training and testing datasets include strides collected in CW, CCW, and SW tasks.

E. Feature Selection and Hyperparameters Tuning

The accuracy of SVR models is heavily affected by input features, kernel function, and hyperparameters (C and ε). Based on our previous work [37], [38], Gaussian kernel function was selected for all SVR models. A Genetic Algorithm (GA) was implemented using RMSE as the cost function to find the best set of features and hyperparameters.

Due to inter-subject variability and differences in the walking condition (CW, CCW, and SW), the traditional k -fold cross-validation method, which relies on randomly splitting observations into k bins, is not a suitable option for feature selection and hyperparameters tuning using GA. Indeed, when we applied the naive k -fold approach during preliminary tests, we obtained clearly overfitted models. For this reason, we implemented a nested leave-one-out cross-validation within the main leave-one-out cross-validation loop. This was done by splitting the training dataset of the main leave-one-out loop into $k = N - 1$ folds (with N being the total number of subjects), each corresponding to a subject included in the training dataset. Then, the SVR model was trained and evaluated k times, each time picking a different subject for evaluation, and the rest for training. For

¹Energy of a time series is defined as the sum over the squared values of the time series data.

²Absolute sum of change returns the sum over the absolute values of subsequent variations in a time series.

TABLE I

The selection ratio of each feature in SVR models. Recurrent features (i.e., selection ratio ≥ 0.7) are marked in bold font.

Features	Stride Length	Stride Velocity	Foot Clearance	Step Length
p^T	1.0	1.0	1.0	–
p^R	1.0	1.0	0	1.0
$ a $	0.5	0.1	0.1	0.5
Stride Time	0	0.5	0.7	0.5
Swing%	0.7	0.1	0.8	0
RMS(a_z)	0.2	0.2	0.2	0.4
RMS(a_{xy})	0.6	0.1	0.4	0.6
$\max(a_z)$	0.2	0.1	0.5	0.1
$\max(a_{xy})$	0.4	0.1	0.5	0.5
$\min(a_z)$	0.1	0.1	0.3	0.2
$\min(a_{xy})$	0.1	0.1	0.4	0
$\text{median}(a_z)$	0.2	0.1	0.2	0.3
$\text{median}(a_{xy})$	0.2	0.1	0.1	0.9
$\text{sum}(a_z)$	0.8	0.4	0.3	0.3
$\text{sum}(a_{xy})$	0.4	0.7	0.1	0.7
$\text{energy}(a_z)$	0.1	0	0.2	0.2
$\text{energy}(a_{xy})$	0.1	0.4	0.4	0.7
$\text{change}(a_z)$	0.5	0.3	0.8	0.3
$\text{change}(a_{xy})$	0.4	0.4	0.4	0.2
$\text{entropy}(a_z)$	0.3	0.2	0.3	0.8
$\text{entropy}(a_{xy})$	0	0	0.8	0.3
Height	0	0.1	0.2	0.1
Weight	0.5	0.4	0.1	0.3
BMI	0.1	0.1	0.2	0.1
Shoe Size	0.2	0.4	0.1	0

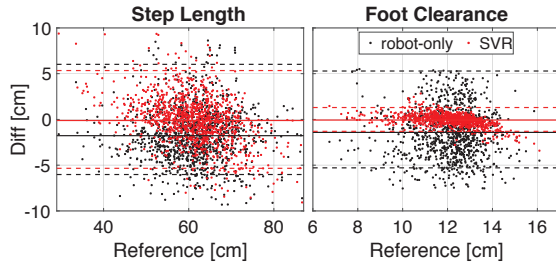


Fig. 5. Bland-Altman plots of step length and foot clearance under two measurement conditions: robot-only and robot-and-insoles with SVR. The y axes represent the difference between estimates and reference data. Limits of agreement are specified as average error (black and red solid lines) $\pm 1.96\text{SD}$ (black and red dashed lines).

a particular choice of features and hyperparameters, the GA cost function was then calculated as the mean of k RMSE scores.

To reduce computational time, we narrowed down the list of candidate hyperparameters values to the following, based on a previous study [37]: $C \in [1 \ 2 \ 5 \ 10 \ 50 \ 100 \ 200]$, $\varepsilon \in [0.1 \ 0.2 \ 0.5 \ 0.8 \ 1 \ 1.5 \ 2 \ 2.5 \ 3]$. Model training and testing were conducted on a 4 GHz Intel® Core™ i7-6700K using MATLAB (The Mathworks Inc., Natick, MA). For each gait parameter, it took less than 30 minutes to train and approximately 0.01 seconds to test the SVR model.

V. RESULTS

Subjects' walking speed varied from 50.2 to 101.7 cm/s (82.2 ± 5.1 cm/s, mean and SD), stride length varied from 77.7 to 134.0 cm (109.2 ± 8.1 cm), foot clearance varied from 10.4 to 17.2 cm (12.9 ± 1.1 cm), step length varied from 38.4 to 68.3 cm (54.5 ± 4.2 cm).

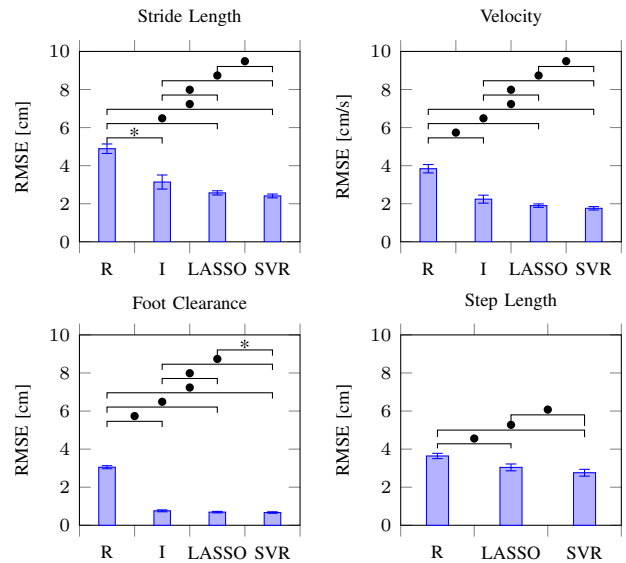


Fig. 6. RMSE of the estimates of stride length, velocity, foot clearance, and step length. R, I, LASSO and SVR represent four measurement conditions: robot-only, insoles-only, insoles-and-robot with LASSO, and insoles-and-robot with SVR. Error bars indicate $\pm 1\text{SE}$. • indicates $p < 0.01$; * indicates $p < 0.05$.

Table I shows the *selection ratio*³ of each feature for the SVR models. The best hyperparameters (C, ε) determined by the GA were (200, 0.5) for SL, SV and ST. For FC, the optimal hyperparameters were (5, 0.1). Figure 5 shows Bland-Altman plots of step length and foot clearance under two measurement conditions: robot-only and robot-and-insoles.

Fig. 6 shows the RMSE and the standard error (SE) of the estimated gait parameters with respect to the ground truth under the four conditions of interest. Wilcoxon signed-rank test was applied to assess significant ($\alpha < 0.05$) differences among the conditions. Bonferroni-Holm method was used to correct for the familywise error rate. Both LASSO and SVR models yielded significantly smaller RMSE than the other two conditions. Additionally, SVR outperformed LASSO in all gait parameters. When used independently, the insoles produced more accurate estimations of stride length, stride velocity and foot clearance than the robot.

VI. DISCUSSION

This paper proposed the use of an autonomous mobile robot and custom-engineered instrumented insoles to conduct gait analysis. The study is motivated by the need for a robot companion to engage older adults in walking exercises, where accurate estimates of the gait parameters are necessary not only to provide feedback to the robot's controller but also to assess the subject's progress (in terms of ambulatory function) longitudinally, across the exercise sessions. We therefore sought to improve accuracy by developing machine

³For each gait parameter, the selection ratio of one feature is defined as the ratio between the number of folds the feature has been selected (in the leave-one-out cross-validation) and the total number of subjects.

learning models to combine data from the robot's on-board RGB-D sensor and from the insoles.

The errors in stride length, stride velocity, foot clearance, and step length were significantly smaller when combining data from the two subsystems (i.e., the robot and the insoles). These estimates also outperformed the accuracy reported in previous studies on the use of wearable sensor or robot's on-board RGB-D sensor to measure gait parameters (Table II). The key benefit of the instrumented insoles lies in their reliable estimates of temporal parameters, which can be directly derived from embedded multi-cell piezoresistive sensors at a fast sample rate (500 Hz). Besides featuring a much slower sample rate (30Hz), Kinect can only approximate the occurrence of gait events based on virtual marker data. Conversely, the key advantages of Kinect relative to the insoles used in this study are the possibility to retrieve consistent, drift-free spatial parameters as well as estimate inter-limb parameters, such as step length, which are associated with adverse outcomes of fall risk in a range of populations [9], [18].

Compared to previous research in mobile gait measurement systems using LRS, the combined models based on SVR yielded more accurate estimates (Table II). For example, Chalvatzaki and colleagues [11], [12] applied Hidden Markov Models to extract stride length from lower-limb movements detected by a robot's on-board LRS, and obtained round to 8.0% mean absolute error. This is likely due to the fact that LRS can only obtain planar information of the leg position at a fixed height [9], as opposed to foot/ankle displacements. Because the ankle plantar-dorsiflexion angle changes during the stance phase of the gait cycle, the position of the foot cannot be directly inferred by tracking the shank. Additionally, LRS might misdetect the subject's legs with other persons' legs, or even tables or chair legs [13], thus making robust detection difficult.

Most of the previous research on the Kinect relied on high degree of freedom skeletal models to track the human body. Although such techniques are capable of extracting foot-level gait parameters, they often suffer from problems of instability, especially with noisy data. Besides, the accuracy of Kinect decreases significantly as the distance between the robot and the subject increases [17], [18]. Furthermore, the performance of the Kinect degrades when occlusions and leg overlapping occur during turns of the subject. Therefore, we implemented SVR models to reduce systematic bias from Kinect data. As expected, SVR outperformed LASSO in all the analyzed gait parameters. This suggests that linear models might oversimplify the underlying relationship between actual gait parameters and raw estimates obtained from the two subsystems. While SVR models proved to be more effective than LASSO models, their accuracy heavily depends on the input features, regularization coefficient, and error margin. For these reasons, we proposed a simple yet effective heuristic method to select input features and tune SVR models. In general, for all the gait parameters, the most relevant features in the SVR models were the raw estimates p^I and p^R (selection ratio 1.0). For stride length, Swing%

TABLE II

The accuracy of stride length (SL), stride velocity (SV), foot clearance (FC), and step length (ST) estimated by different systems. The last row presents the results of our proposed SVR model and fusion algorithm.

Ref.	System	Task	MAE%			
			SL	SV	FC	ST
[29]	IMU	Straight	7.8%	—	—	—
[25]	IMU	Straight	>2.0%	—	>4.0%	—
[49]	IMU	Straight	>2.0%	—	>4.0%	—
[24]	IMU	Curve	>2.0%	>2.0%	>7.5%	—
[14]	RGB-D	Straight	—	>3.0%	—	>4.0%
[13]	RGB-D	Straight	2.0%	—	—	—
[9]	LRS	Straight	—	—	—	>8.0%
[11]	LRS	Straight	8.0%	—	—	—
[34]	IMU+LRS	Curve	—	2.0%	—	—
SVR	IMU+RGB-D	Curve	1.5%	1.4%	4.0%	3.4%

and $\text{sum}(a_z)$ were also recurrent features. This suggests that stride length correlates with the duration of the swing phase and with the vertical acceleration of the foot at push-off and heel-strike (intuitively, longer strides imply longer swing periods and larger propulsive and braking forces [47], [48]). Stride velocity can be computed as the integral of the horizontal acceleration of the foot over time, thereby explaining the correlation found with $\text{sum}(a_{xy})$. For step length, it is worth noting that SVR models did not include the raw estimates from the insoles because these in-foot devices cannot measure spatial inter-limb parameters. The modest accuracy of the Kinect sensor in measuring linear displacements becomes apparent when such displacements are relatively small, as in case of the foot clearance (Fig. 5). Indeed, the Kinect estimates for this parameter did not correlate well with the ground-truth values. Interestingly, the anthropometric features were not consistently included in the optimal set of features. This is likely due to the limited heterogeneity of the study sample.

VII. CONCLUSION

This paper presented the design of a mobile gait measurement system consisting of an autonomous mobile robot equipped with an RGB-D sensor and instrumented insoles. We focused on the validation of the system as a tool to measure clinically meaningful stride-to-stride kinematic gait parameters during straight walking and turning. Results confirmed our hypothesis that the combined use of robot RGB-D sensor and in-shoe sensors increases the accuracy of the gait estimates, and that machine learning models (i.e., the SVR method) are more effective than linear models (i.e., the LASSO method) in reducing systematic errors in the estimates. It is worth noting that the proposed methods do not rely on subject-specific training data, and therefore can be applied even without the need for a reference system to collect ground-truth data. Future work includes validating the proposed methods in extended-time measurements with a heterogeneous group of participants (e.g., older adults with gait disorders). The developed system will be further used to engage older adults in walking exercises with gait parameter monitoring and progress assessment.

REFERENCES

[1] J. E. Ahlskog, Y. E. Geda, N. R. Graff-Radford, and R. C. Petersen, "Physical exercise as a preventive or disease-modifying treatment of dementia and brain aging," in *Mayo Clinic Proceedings*, vol. 86, no. 9, 2011, pp. 876–884.

[2] A. A. Ayler, R. C. Brownson, S. J. Bacak, and R. A. Housemann, "The epidemiology of walking for physical activity in the United States," *Medicine & Science in Sports & Exercise*, vol. 35, no. 9, pp. 1529–1536, 2003.

[3] J. N. Morris and A. E. Hardman, "Walking to health," *Sports Medicine*, vol. 23, no. 5, pp. 306–332, 1997.

[4] W. H. Organization, *World Report on Ageing and Health*, 2015.

[5] M. Montero-Odasso, M. Schapira, E. R. Soriano, M. Varela, R. Kaplan, L. A. Camera, and L. M. Mayorga, "Gait velocity as a single predictor of adverse events in healthy seniors aged 75 years and older," *The Journals of Gerontology Series A: Biological Sciences and Medical Sciences*, vol. 60, no. 10, pp. 1304–1309, 2005.

[6] L. Z. Rubenstein, "Falls in older people: epidemiology, risk factors and strategies for prevention," *Age and Ageing*, vol. 35, no. suppl.2, pp. ii37–ii41, 2006.

[7] G. L. Maddox, *The Encyclopedia of Aging: A Comprehensive Resource in Gerontology and Geriatrics*. Springer, 2013.

[8] J. Verghese, R. Holtzer, R. B. Lipton, and C. Wang, "Quantitative gait markers and incident fall risk in older adults," *The Journals of Gerontology: Series A*, vol. 64, no. 8, pp. 896–901, 2009.

[9] C. Piezzo, B. Leme, M. Hirokawa, and K. Suzuki, "Gait measurement by a mobile humanoid robot as a walking trainer," in *IEEE International Symposium on Robot and Human Interactive Communication*, 2017, pp. 1084–1089.

[10] A. Yorozu and M. Takahashi, "Development of gait measurement robot using laser range sensor for evaluating long-distance walking ability in the elderly," in *IEEE/RSJ International Conference on Intelligent Robots and Systems*, 2015, pp. 4888–4893.

[11] X. S. Papageorgiou, G. Chalvatzaki, K.-N. Lianos, C. Werner, K. Hauer, C. S. Tzafestas, and P. Maragos, "Experimental validation of human pathological gait analysis for an assisted living intelligent robotic walker," in *IEEE International Conference on Biomedical Robotics and Biomechatronics*, 2016, pp. 1086–1091.

[12] G. Chalvatzaki, X. S. Papageorgiou, and C. S. Tzafestas, "Towards a user-adaptive context-aware robotic walker with a pathological gait assessment system: First experimental study," in *IEEE/RSJ International Conference on Intelligent Robots and Systems*, 2017, pp. 5037–5042.

[13] V. Bonnet, C. A. Coste, L. Lapierre, J. Cadic, P. Fraisse, R. Zapata, G. Venture, and C. Geny, "Towards an affordable mobile analysis platform for pathological walking assessment," *Robotics and Autonomous Systems*, vol. 66, pp. 116–128, 2015.

[14] B. Jaschke, A. Vorndran, T. Q. Trinh, A. Scheidig, H.-M. Gross, K. Sander, and F. Layher, "Making gait training mobile - a feasibility analysis," in *IEEE International Conference on Biomedical Robotics and Biomechatronics*, 2018.

[15] T. Pallejà, M. Teixidó, M. Tresanchez, and J. Palacín, "Measuring gait using a ground laser range sensor," *Sensors*, vol. 9, no. 11, pp. 9133–9146, 2009.

[16] M. Gabel, R. Gilad-Bachrach, E. Renshaw, and A. Schuster, "Full body gait analysis with Kinect," in *Annual International Conference of the IEEE Engineering in Medicine and Biology Society*, 2012, pp. 1964–1967.

[17] E. Stone and M. Skubic, "Evaluation of an inexpensive depth camera for in-home gait assessment," *Journal of Ambient Intelligence and Smart Environments*, vol. 3, no. 4, pp. 349–361, 2011.

[18] R. A. Clark, K. J. Bower, B. F. Mentiplay, K. Paterson, and Y.-H. Pua, "Concurrent validity of the Microsoft Kinect for assessment of spatiotemporal gait variables," *Journal of Biomechanics*, vol. 46, no. 15, pp. 2722–2725, 2013.

[19] K. O. Arras, S. Grzonka, M. Luber, and W. Burgard, "Efficient people tracking in laser range data using a multi-hypothesis leg-tracker with adaptive occlusion probabilities," in *IEEE International Conference on Robotics and Automation*, 2008, pp. 1710–1715.

[20] A. Yorozu, T. Moriguchi, and M. Takahashi, "Improved leg tracking considering gait phase and spline-based interpolation during turning motion in walk tests," *Sensors*, vol. 15, no. 9, pp. 22 451–22 472, 2015.

[21] R. Y.-C. Tsai, H. T.-Y. Ke, K. C.-J. Lin, and Y.-C. Tseng, "Enabling identity-aware tracking via fusion of visual and inertial features," in *International Conference on Robotics and Automation*, 2019, pp. 2260–2266.

[22] S. Khan and M. Shah, "Tracking people in presence of occlusion," in *Asian Conference on Computer Vision*, vol. 5, 2000.

[23] N. Hegde, M. Bries, and E. Sazonov, "A comparative review of footwear-based wearable systems," *Electronics*, vol. 5, no. 3, p. 48, 2016.

[24] B. Mariani, C. Hoskovec, S. Rochat, C. Büla, J. Penders, and K. Aminian, "3D gait assessment in young and elderly subjects using foot-worn inertial sensors," *Journal of Biomechanics*, vol. 43, no. 15, pp. 2999–3006, 2010.

[25] S. Minto, D. Zanotto, E. M. Boggs, G. Rosati, and S. K. Agrawal, "Validation of a footwear-based gait analysis system with action-related feedback," *IEEE Transactions on Neural Systems and Rehabilitation Engineering*, vol. 24, no. 9, pp. 971–980, 2016.

[26] B. Mariani, M. C. Jiménez, F. J. Vingerhoets, and K. Aminian, "On-shoe wearable sensors for gait and turning assessment of patients with Parkinson's disease," *IEEE Transactions on Biomedical Engineering*, vol. 60, no. 1, pp. 155–158, 2012.

[27] D. Zanotto, E. M. Mamuyac, A. R. Chambers, J. S. Nemer, J. A. Stafford, S. K. Agrawal, and A. K. Lalwani, "Dizziness handicap inventory score is highly correlated with markers of gait disturbance," *Otolaryngology*, vol. 38, no. 10, pp. 1490–1499, 2017.

[28] J. Montes, D. Zanotto, S. Dunaway Young, R. Salazar, D. C. De Vivo, and S. Agrawal, "Gait assessment with SoleSound instrumented footwear in spinal muscular atrophy," *Muscle & Nerve*, vol. 56, no. 2, pp. 230–236, 2017.

[29] A. Rampp, J. Barth, S. Schülein, K.-G. Gaßmann, J. Klucken, and B. M. Eskofier, "Inertial sensor-based stride parameter calculation from gait sequences in geriatric patients," *IEEE Transactions on Biomedical Engineering*, vol. 62, no. 4, pp. 1089–1097, 2015.

[30] N. Hegde, T. Zhang, G. Uswatte, E. Taub, J. Barman, S. McKay, A. Taylor, D. M. Morris, A. Griffin, and E. S. Sazonov, "The pediatric SmartShoe: wearable sensor system for ambulatory monitoring of physical activity and gait," *IEEE Transactions on Neural Systems and Rehabilitation Engineering*, vol. 26, no. 2, pp. 477–486, 2017.

[31] J. M. Hausdorff, Z. Ladin, and J. Y. Wei, "Footswitch system for measurement of the temporal parameters of gait," *Journal of Biomechanics*, vol. 28, no. 3, pp. 347–351, 1995.

[32] J. Ziegler, H. Kretzschmar, C. Stachniss, G. Grisetti, and W. Burgard, "Accurate human motion capture in large areas by combining IMU-and laser-based people tracking," in *IEEE/RSJ International Conference on Intelligent Robots and Systems*, 2011, pp. 86–91.

[33] G. Li, C. Zhu, J. Du, Q. Cheng, W. Sheng, and H. Chen, "Robot semantic mapping through wearable sensor-based human activity recognition," in *IEEE International Conference on Robotics and Automation*, 2012, pp. 5228–5233.

[34] C. A. Cifuentes, A. Frizera, R. Carelli, and T. Bastos, "Human–robot interaction based on wearable IMU sensor and laser range finder," *Robotics and Autonomous Systems*, vol. 62, no. 10, pp. 1425–1439, 2014.

[35] R. O. Duda, P. E. Hart, and D. G. Stork, *Pattern Classification*. John Wiley & Sons, 2012.

[36] H. Zhang, D. Zanotto, and S. K. Agrawal, "Estimating COP trajectories and kinematic gait parameters in walking and running using instrumented insoles," *IEEE Robotics and Automation Letters*, vol. 2, no. 4, pp. 2159–2165, 2017.

[37] H. Zhang, M. O. Tay, Z. Suar, M. Kurt, and D. Zanotto, "Regression models for estimating kinematic gait parameters with instrumented footwear," in *IEEE RAS/EMBS International Conference on Biomedical Robotics and Biomechatronics*, 2018.

[38] H. Zhang, Y. Guo, and D. Zanotto, "Accurate ambulatory gait analysis in walking and running using machine learning models," *IEEE Transactions on Neural Systems and Rehabilitation Engineering*, 2019.

[39] Kinect for windows sdk 2.0. [Online]. Available: [https://docs.microsoft.com/en-us/previous-versions/windows/kinect/dn799271\(v=ieb.10\)](https://docs.microsoft.com/en-us/previous-versions/windows/kinect/dn799271(v=ieb.10))

[40] P. Leica, J. M. Toibero, F. Roberti, and R. Carelli, "Switched control to robot-human bilateral interaction for guiding people," *Journal of Intelligent & Robotic Systems*, vol. 77, no. 1, pp. 73–93, Jan 2015. [Online]. Available: <https://doi.org/10.1007/s10846-014-0098-6>

[41] J. Elson, L. Girod, and D. Estrin, "Fine-grained network time synchronization using reference broadcasts," *ACM SIGOPS Operating Systems Review*, vol. 36, no. SI, pp. 147–163, 2002.

[42] T. Hastie, R. Tibshirani, and J. Friedman, *The elements of statistical learning: data mining, inference, and prediction*. Springer Science & Business Media, 2009.

- [43] J. Friedman, T. Hastie, and R. Tibshirani, "Regularization paths for generalized linear models via coordinate descent," *Journal of Statistical Software*, vol. 33, no. 1, p. 1, 2010.
- [44] F. Huxham, J. Gong, R. Baker, M. Morris, and R. Iansek, "Defining spatial parameters for non-linear walking," *Gait & Posture*, vol. 23, no. 2, pp. 159–163, 2006.
- [45] I. Skog, P. Handel, J.-O. Nilsson, and J. Rantakokko, "Zero-velocity detection algorithm evaluation," *IEEE Transactions on Biomedical Engineering*, vol. 57, no. 11, pp. 2657–2666, 2010.
- [46] A. Ferrari, P. Ginis, M. Hardegger, F. Casamassima, L. Rocchi, and L. Chiari, "A mobile Kalman-filter based solution for the real-time estimation of spatio-temporal gait parameters," *IEEE Transactions on Neural Systems and Rehabilitation Engineering*, vol. 24, no. 7, pp. 764–773, 2015.
- [47] J. Perry, J. R. Davids *et al.*, "Gait analysis: normal and pathological function," *Journal of Pediatric Orthopaedics*, vol. 12, no. 6, p. 815, 1992.
- [48] T. F. Novacheck, "The biomechanics of running," *Gait & Posture*, vol. 7, no. 1, pp. 77–95, 1998.
- [49] N. Kitagawa and N. Ogihara, "Estimation of foot trajectory during human walking by a wearable inertial measurement unit mounted to the foot," *Gait & Posture*, vol. 45, pp. 110–114, 2016.